INDIAN JOURNAL OF SCIENCE AND TECHNOLOGY

ORIGINAL ARTICLE

OPEN ACCESS

Received: 10/12/2025

Accepted: 23/12/2025

Published: 31/12/2025

Citation: Marathe MS, Deshmukh V (2025) Comparative Study of Cartesian and Polar 3D Printer Architectures by Mathematical Modelling. Indian Journal of Science and Technology 18(48): 3937-3945. https://doi.org/10.17485/IJST/v18i48.183

* **Corresponding author**.

marathemayu1990@gmail.com; mayur.marathe@nmims.edu

Funding: None

Competing Interests: None

Copyright: © 2025 Marathe & Deshmukh. This is an open access article distributed under the terms of the Creative Commons Attribution License, which permits unrestricted use, distribution, and reproduction in any medium, provided the original author and source are credited.

Published By Indian Society for Education and Environment (iSee)

ISSN
Print: 0974-6846
Electronic: 0974-5645

Comparative Study of Cartesian and Polar 3D Printer Architectures by Mathematical Modelling

Mayur S Marathe[1]*, Venkatesh Deshmukh[1]

1 Department Of Mechanical Engineering, Mukesh Patel School of Technology Management & Engineering, SVKM's NMIMS, Mumbai, India

Abstract

Objectives: To develop a unified math model for Cartesian and Polar printers that are driven by hybrid polar stepper motors. The aim is to perform a comparative analysis in terms of model complexity and motion behavior. **Methods:** This study highlights the area of research, focusing on the development of comprehensive mathematical models for Cartesian and polar 3D printers driven by a hybrid bipolar stepper motor. This approach develops axis-level modeling along with subsystems such as the stepper motor. This study takes the first steps toward developing a digital twin that enables real-time simulation and adaptive control for the next generation of 3D printers. **Findings:** The nonlinear differential equation ensures a high-fidelity representation of the real-world dynamics. In the case of a Cartesian printer, the model uses a simple linear kinematic equation for decoupled X-Y-Z motion. On the contrary, in the case of a polar printer, it introduces a nonlinear coupled inverse kinematic relation between radial (R) and angular axis (Θ). **Novelty:** By developing a unified nonlinear electrotechnical model for Cartesian and polar printers, it enables high-fidelity dynamics without linearization. It forms the base of digital twin technology and extends towards next-generation additive manufacturing systems.

Keywords: Cartesian 3D Printer; Polar 3D Printer; Unified Modelling; Digital twin; Comparative analysis

1 Introduction

3D printer has developed and gained market share in recent times, which has led to the evolution of 3D printers in a short span. This evolution was primarily for Fuse Depositional Modelling (FDM) -based 3D printers, which have a stepper motor for individually controlling the motion of the print head in all axes. For obtaining a good quality of print, the positioning of the print head for each instance is crucial. The expansion of Additive manufacturing (AM) results in varied printer configurations where polar and Cartesian 3D printers play an important role. Due to the simplicity and reliability of the Cartesian configuration, which is characterized by orthogonal X

-Y-Z motion, it is mainly adopted. In contrast, the polar configuration has radial and angular co-ordinates, i.e., R, Θ, and Z, which provide an upper hand in circular motion, which has nonlinearities in control and modelling. The study of mathematical modelling, which examines how an electric motor behaves under different conditions, such as electrical, mechanical, and electrotechnical, is referred to as motor dynamics. It gives us an understanding of how the motor will behave for the given input (voltage, current) and external influences over a period of time. The integration of motor dynamics with various mechanical assemblies was studied by Marathe et al.[(1)] They use a sin-cos micro-stepping voltage pulse to get a trapezoidal profile. They also include the speed-up factor for generating the motion profile. Rojek et al.[(2)] emphasized the use of AI to enhance predictive maintenance and process simulation for the digital twins (DT), which enables anomaly detection and closed-loop control. Mourtzis et al.[(3)] developed a DT framework for a Cartesian 3D printer, which fuses sensor feedback to adjust process parameters and improve quality. In 2018, Yin et al.[(4)] conducted an investigation into dynamic modeling for the motion of a Cartesian printer, highlighting the use of a timing belt for precise positioning of the print head at high speeds. The author aims on identifying the error in positioning the print head due to belt elasticity. The author also proposes alternate technique to predict positioning error in various operating conditions.

A comparative study was carried out using Finite Element Analysis (FEA). by Raj et al.[(5)] to asses surface roughness and material deformation for Cartesian and polar printers, the conclusion was made that for Cartesian systems, carbon fiber is optimal, and structural steel is optimal for polar printers. In 2022 Bernardi et al.[(6)] for hybrid stepper motors compared to current control strategies, which include sliding mode, Proportional-Integral (PI), and predictive control. Due to this finding, the efficiency of closed-loop control is improving. To estimate the natural frequencies, Kopets et al.[(7)] use Euler–Lagrange formalism for Cartesian printers, aiding vibration analysis and design optimization.

Cao et al.[(8)] presented a strategy that considers fuzzy Pi and Sliding Motor Control (SMC) to enhance the precision and surface quality in a fused deposition modeling printer. Based on the system condition, their adaptive mechanism dynamically adjusted the control weights to reduce the overall defects. This study makes a significant contribution to the development of control strategies. In 2024, a study was carried out to compare the dynamic stability and structural integrity of widely used 3D printers, which are Cartesian, Polar, and Delta, by Tyagi et al.[(9)] with the help of FEA. The author discusses the impact of structural behavior on precision and quality. For real-time monitoring and optimization of 3D printing, the technology of DT has increased. Palanisamy et al.[(10)] discusses how different process parameters and material selection affect the printing quality of FDM printers. The author employs the Design of Experiments (DOE), Taguchi method, (ANOVA), Response surface methodology (RSM), and AI approach to conclude optimized strategies. Dynamic modeling has evolved with the Lagrangian approach. The Finite Element Method (FEM) is used for accurate vibrational analysis and control. Mishra et al.[(11)] highlight the coupling effect, configuration-dependent natural frequencies, and computational trade-offs. Simpkins et al.[(12)] emphasize adaptive algorithms, robust timing analysis, and watchdog systems to ensure the safety and stability of the humanoid robot. Tlegenov et al.[(13)] studied condition monitoring for the current-based nozzle 3D printer. The author derived the extrusion force and validated the motor current in a clogging condition, which was validated by experimental analysis using Polylactic Acid (PLA).

The Delta kinematics printer offers cost benefits and speed advantages over Cartesian systems. The study highlighted the advantages in surface quality. Zakharov et al.[(14)] focused their paper on performance enhancement through kinematic modeling, trajectory optimization, and structural improvement. Zhao et al.[(15)] employed a neural network for data-driven approximation, utilizing experimental datasets to ehance trajectory tracking and robustness for the Delta 3D printer. In comparison to the traditional model, the neural approach enhances control accuracy in diverse conditions. Chouaibi et al.[(16)] studied the Ultimaker-style FDM printer to understand the effect of joint clearance. A coordinate measuring machine is used to compare deviations in printed artifacts.

Savaliya et al.[(17)] Define the relationship between the joint parameter and print head position using kinematic modeling in an FDM printer. Forward kinematics help determine the position of the end-effector for a given joint angle, whereas inverse kinematics give the joint angle for a desired position. Inverse kinematics for manipulators is complex due to the nonlinearity involved. Bouzid et al.[(18)] Employ smart techniques such as Artificial Neural Networks (ANNs), adaptive neuro-fuzzy inference system (ANFIS), and deep learning to achieve accuracy and efficiency for the Selective Compliance Articulated Robotic Arm (SCARA) robot. To overcome the limitations of the Cartesian and the delta printer, multi- Degree of freedom (DOF) arms are integrated. Xu et al.[(19)] emphasize inverse kinematics, trajectory planning, and motion interpolation for stability and precision. Xie et al.[(20)] Employ a position-posture separation method for the inverse kinematics of a robotic arm, utilizing a 3D printer. It decouples the nonlinear equation by using the geometric method and the analytical method. Alba et al.[(21)] compare toll path patterns using counter parallel and Hilbert curve in additive manufacturing for improvement in smoothness and connectivity. The author analyzed print time, material length, underfill, etc., for the modified contour parallel path, along with reduced material usage with Hilbert-based patterns. In large-scale additive manufacturing Liu et al.[(22)] in his paper introduce continuous path planning method combining spiral wall and zigzag fill paths. This method improves molding accuracy, uniform temperature, etc., due to which it offers significant advantages for industrial fabrication. Gupta et al.[23] optimize large scale 3D printing tool path using the Space-Filling Curve Based Domain Decomposition (SFCDcomp) framework. The author experimented on complex models, which shows a significant strength difference with varying overlap strategies. An integrated study of a mathematical model & 3D printer, and software optimization to control the extruder is available[24]. A large study is available in the perspective of material deposition rate[25] and process parameter[26] is available, but the mechanism of motion modelling for the integrated model, which includes mechanized assembly of motors, gearbox, is yet to be explored.

1.1 Research Gap

Several studies focused on separate modeling approaches, control strategies, DT, predictive maintenance, material, and structural analysis. But the research gap lies in the integrated math model, which combines both mechanical and electrical dynamics for a unified model of a 3D printer. Past research data detail with domain separately, which limits the ability to anticipate the behavior and motion of the printer in actual operating conditions.

1.2 Problem Statement

Positioning of the print head is important to achieve for high quality prints, specifically in an FDM printer where the stepper motor governs multiple axes. Numerous studies address motor dynamics, control strategies, and mechanical assemblies, but lack in integrated modelling approach, which creates a challenge in comparing configurations to guide design optimization for emerging printer architectures.

2 Methodology

In order to understand the dynamic behavior, optimal performance, and effective control over the positioning of the Cartesian and Polar configured printer, mathematical modelling is essential. In this section discuss the framework of the unified model, which integrates electromechanical components in both configurations with nonlinear differential equations. Core components are stepper motors, timing belt, gearbox, timing belt, power screw, turning table, and rack and pinion assembly. Mathematical representation for core electrical & mechanical components refers to a unified model

2.1 Unified Modelling Philosophy

Hybrid bipolar stepper motor actuates core 3D printer and couple mechanically for the motion mechanism in which either print head drive for Cartesian motion or the turn-table for polar motion to convert electrical signals to controlled displacement. In case of unified mechatronic perspective, the system is considered as a single chain where voltage pulse is the input (often implemented as micro-stepping voltage pulse) and axis displacement is the output (position/velocity). The way in which the printer is modelled supports both open loop operation (pulse to position without feedback) and closed loop where feedback signals (e.g., position, speed, current or load estimates) are utilized to reduce error and improve disturbance rejection. The mathematical model is developed: first nonlinear differential equation describes the motor dynamics (phase currents, resistance/inductance effects, back EMF) and mechanical dynamics (torque generation, rotor inertia, damping, detent torque, and load torque interaction). Next are the required mechanical components such as gearbox, timing belt-pulley, rack and pinion, lead screw or tuning table are modelled and interconnected according to printer's requirement. In the end, kinematics relationships map rotary motion of motor to travel in X, Y, Z or θ, preserving nonlinearities to achieve high fidelity simulation for controller design and DT development. Below figure 1 (a) and (b) represents unified model for Cartesian and Polar configuration 3D printer.

2.2 Component Level Modelling

Component-level modelling represents building a mathematical description for each mechanical element of the 3D printer separately before defining them into one unified model. In place of treating a printer as a single black box, each and every subsystem i.e., motor, belt, screw, gearbox, load and bearings is represented by its own governing equations and parameters. This approach makes easy to validate each part, identify dominant dynamics, and reuse blocks across different printer architectures. This section restricts to the stepper motor, capturing its electrical and mechanical behaviour via nonlinear differential equations.

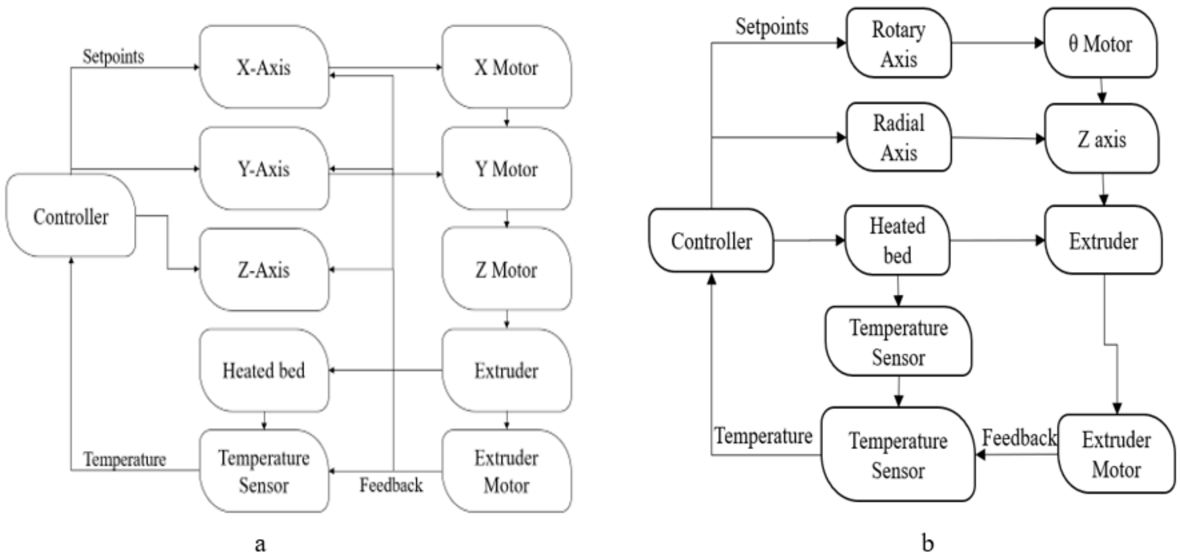

Fig 1. a. Unified model of Cartesian 3D printer, b. Unified model of Polar 3D printer

2.2.1. Stepper motor model

The non-linear electromechanical differential equation is modelled for a hybrid bipolar stepper motor[1]. The motor is governed by two phases (A and B) and its dynamics are governed by the equation 1,2,3 and 4 given below:

$$\frac{di_a}{dt} = \frac{-R_a i_a + K_b \theta_m \sin(N_r \theta_m)}{L_a} + \frac{V_A(t)}{L_a} \tag{1}$$

$$\frac{di_b}{dt} = \frac{-R_a i_b + K_b \theta_m \cos(N_r \theta_m)}{L_a} + \frac{V_B(t)}{L_a} \tag{2}$$

$$T_m(t) = -K_T i_a \sin(N_r \theta_m) + K_T i_b \cos(N_r \theta_m) \tag{3}$$

$$\frac{d\theta_m}{dt} = \frac{T_m(t) - D_m \theta_m - K_D \sin(4N_r \theta_m)}{J_m} - \frac{T_{R\perp}(t)}{J_m} \tag{4}$$

Notations are as follows,

$\theta_m(t) =$ shaft rotation of motor in radians, $\theta_m(t) =$ Rotational velocity in radians/s, $L_a, R_a =$ phase inductance in Henry and resistance in Ohm for the two phases A and B, $K_T =$ Torque, $K_B =$ Back EMF constants, $K_D =$ Detent Torque constant, $T_m(t) =$ motor torque in Nm, $T_{R1}(t) =$ load torques in Nm, $i_A(t)/i_B(t) =$ phase currents in Ampere, $V_A(t)/V_B(t) =$ phase voltages in Volts, respectively, $N_r =$ number of rotor teeth, $J_m =$ Rotor polar mass moment of inertia $(kg \cdot m^2)$, $Dm =$ torsional viscous damping coefficient (Ns/m).

The above equations 1-a and 1-b describe how armature current i_a and i_b change with respect to time. The equation 1-d, i.e.: $T_m(t)$ is the equation of torque for two phase hybrid bipolar stepper motor. Incorporating back EMF and detent torque, the motor torque is generated, which is a function of phase current and rotor position.

The equation 1-e i.e.: $\frac{d\dot{\theta}_m}{dt}$ represents the angular acceleration of the rotor, which depends upon the load torque of the mechanism.

2.2.2. Cartesian Configuration

Motion in each axis (X, Y, Z) is independently controlled. Modelling of each axis is done independently due to the decoupled nature of Cartesian kinematics. The torque output from one component is the input to the next, which leads to the derivation of an equation for each axis. The stepper motor, gearbox & timing belt is the unified model for the Cartesian printer in X & Y directions. For Z direction stepper motor, gearbox, and power screw give the unified model. Figure 2(a) represent the X-, Y-axis and Figure 2(b) Z-axis mechanisms for cartesian printer.[14]

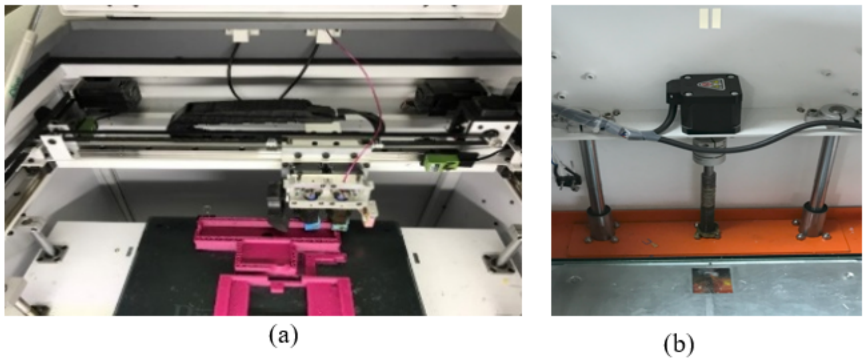

Fig 2. (a) X-axis Mechanism and Y-axis Mechanism (b) Z-axis Mechanism

In X and Y motion, the unified equation is obtained by substituting the kinematic relationship $\theta(t)=\theta_2(t)=\frac{r_1}{r_2}\theta_1(t)=\frac{r_1}{r_2}\theta_m(t)$. The torque of the timing belt, which, after simplification, is substituted in the equation of the gearbox to get $T_{R1}(t)$ as shown below[1] by equation 5.

$$\begin{aligned}&\left[J_{o1}^{gb}+J_{o2}^{gb}\left(\frac{r_\perp}{r_2}\right)^2\right]\ddot{\theta}_m+\left[D_1^{gb}+D_2^{gb}\left(\frac{r_\perp}{r_2}\right)^2\right]\dot{\theta}_m\\&+\left[(J_{o1}^{tb}+J_{o2}^{tb}+mr^2)\ddot{\theta}_m+(D_1^{tb}+D_2^{tb})\dot{\theta}_m+m^{tb}gr\sin a\right]\left(\frac{r_\perp}{r_2}\right)^2=T_{R1}(t)\end{aligned} \tag{5}$$

The above equation is finally substituted in equation (1-e) to get the angular acceleration of the rotor.

In Z-axis motion, the unified equation is obtained by replacing the input torque of the screw in the equation of the gearbox to get $T_{R1}(t)$ as shown below[1] by equation 6.

$$\begin{aligned}&\left[J_{o1}^{gb}+J_{o2}^{gb}\left(\frac{r_\perp}{r_2}\right)^2\right]\ddot{\theta}_m+\left[D_1^{gb}+D_2^{gb}\left(\frac{r_\perp}{r_2}\right)^2\right]\dot{\theta}_m+\left[J^{ps}\frac{\lambda}{2\pi}\ddot{\theta}_m\right.\\&\left.+G(\mu,\alpha)\left(m^{ps}\frac{\lambda}{2\pi}\ddot{\theta}_m+m^{ps}g+D^{ps}\frac{\lambda}{2\pi}\dot{\theta}_m\right)r_{sc}\right]\left(\frac{r_\perp}{r_2}\right)^2=T_{R1}(t)\end{aligned} \tag{6}$$

The above equation is finally substituted in equation (1-e) to get the angular acceleration of the rotor.

2.2.3. Polar configuration

The unified model motion for the polar printer is R, Θ, Z direction motions are derived. The Stepper motor, Gearbox, and Rack & pinion refer to a unified model for R direction motion. The Stepper motor, Gearbox, and Turning Table refer to a unified model for Θ direction motion. And the Stepper motor, Gearbox & Power screw refer to a unified model for Z direction motion. Figure 3 shows the symbolic diagram of a Polar printer[2]. Just like cartesian configuration, the polar gives a nonlinear kinematic relationship between the motor inputs and cartesian workspace coordinates.

For R-axis motion, the unified equation is obtained by combining the Rack & Pinion equation of motion with the gearbox equation of motion, which, after simplification, is obtained[2] as stated in equation 7,

$$\left[J_{o1}^{gb}+J_{o2}^{gb}\left(\frac{r_\perp}{r_2}\right)^2\right]\ddot{\theta}_m+\left[D_1^{gb}+D_2^{gb}\left(\frac{r_\perp}{r_2}\right)^2\right]\dot{\theta}_m+\left[\left(\frac{3}{2}m^{rp}r_p^2\right)\ddot{\theta}_m+(D^{rp})\right]\dot{\theta}_m\left(\frac{r_\perp}{r_2}\right)^2=T_{R1}(t) \tag{7}$$

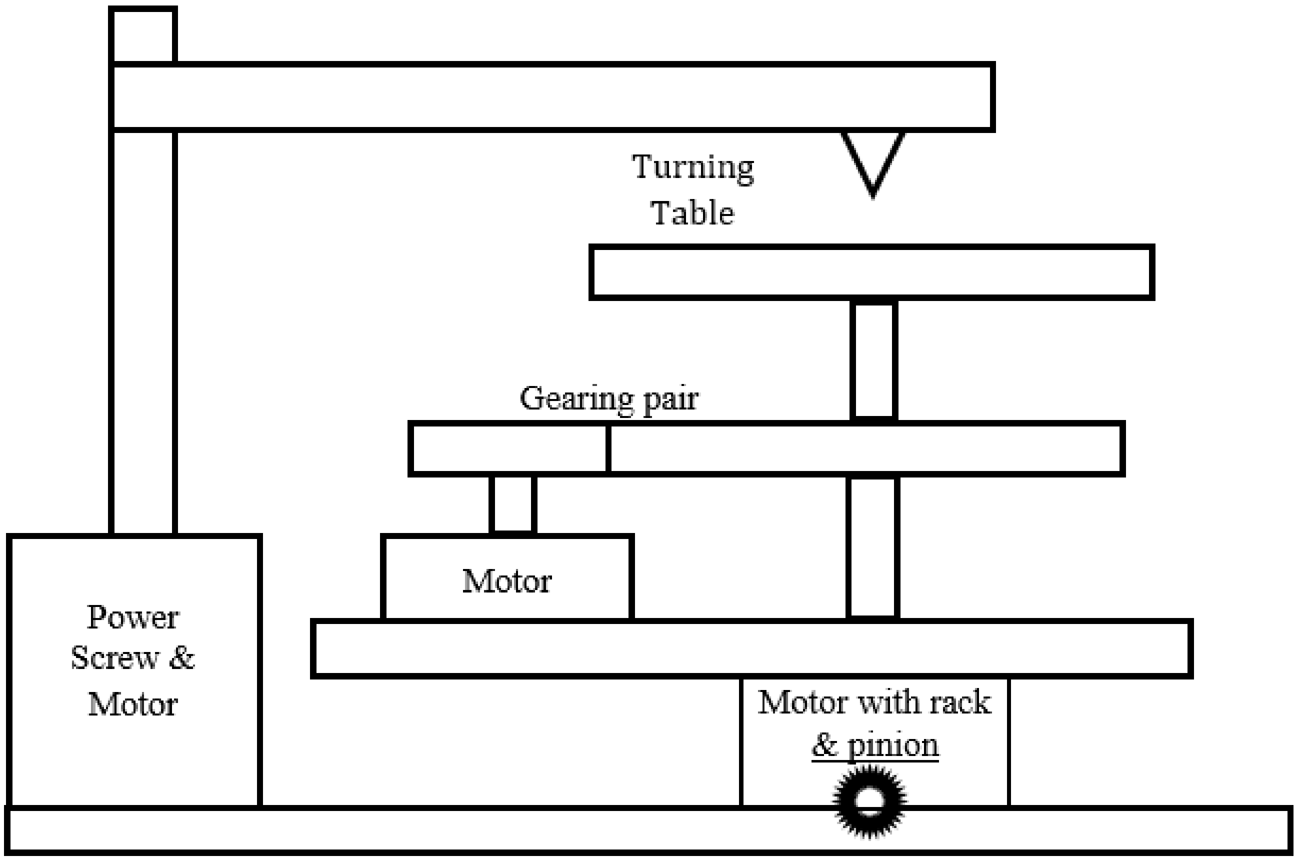

Fig 3. Symbolic representation of a polar configuration 3D Printer

For Θ-axis motion, the unified equation is obtained by substituting the equation of motion for a turntable with the gearbox equation of motion, which, after simplification, is obtained [2] as stated in equation 8,

$$\left[J_{o1}^{gb} + J_{o2}^{gb}\left(\frac{r_1}{r_2}\right)^2\right]\ddot{\theta}_m + \left[D_1^{gb} + D_2^{gb}\left(\frac{r_1}{r_2}\right)^2\right]\dot{\theta}_m + \left[J^{tt}\ddot{\theta}_m + D^{tt}\dot{\theta}_m\right]\left(\frac{r_1}{r_2}\right)^2 = T_{R1}(t) \tag{8}$$

And finally, for Z-axis motion, the unified model for polar and Cartesian configuration is the same. The small difference we observe is that in polar head moves and in Cartesian printing table moves.

3 Result and discussion

The unified model is suitable as a Digital twin because it develops a mechatronic relation from voltage pulse (micro stepping pulse) to axis displacement outputs while preserving nonlinear electromechanical dynamics and load interactions. Integrating motor, gearbox and transmission subsystem in axis level models enables time domain simulation in both open and close loop operation, supporting real time prediction and orientation study. Furthermore, this comparative analysis of computational indicated that Cartesian DT [4] can run efficiently due to decoupled linear kinematics, whereas polar DT [7] remain feasible but requires more computation because of nonlinear inverse kinematics and synchronized multivariable control.

Comparative study aligns with previous research work in additive manufacturing and motion modelling. A study says that the Cartesian printer exhibits superior linear positioning accuracy because of a decoupled X-Y-Z motion structure. A researcher Yin et al. [4], reports that because of simple kinematic mapping and timing belt mechanism, the cartesian achieve high precision in straight line trajectories. Kopets et al. [7] highlight dynamic behaviour for Cartesian printers that supports the current model conclusion on reduced compactional complexity.

Tyagi et al.[9] say that polar printers excel in circular and radial patterns but have nonlinearities and coupling effects due to increased complexity in structural behaviours and control strategies. The inverse kinematics and multi-variable control are derived in this study for the polar printer, which is also supported by Bouzid et al.[18], who demonstrated the computational challenges in robotics arms with similar kinematic dependencies. Comparative analysis based on mathematical approach, model complexity, and print pattern complexity shows the influence of dynamic error for both systems. The findings validate the importance of an integrated model to predict the motion behaviour and optimize control strategies.

3.1 Mathematical approach

In additive manufacturing, the Cartesian printer or Polar 3D printer have influencing factor for design, control, and performance. This rigorous study for comparative analysis based on mathematical modelling complexity provides a base of understanding for selecting the appropriate configuration for selective applications. By integrating electrical and mechanical components into a single model, it enables the high-fidelity simulation of actual-world printing manoeuvres. This modelling foundation is instrumental for DT development, controller design, and performance optimization in a 3D printing system.

In Cartesian configuration nonlinear differential equation derived from elector mechanical models of the models controls each axis. Due to linear kinematic relationships between motor and print head displacement, the equations are relatively straightforward. For instance, in timing belt assembly, rotational motion is converted into linear displacement with a constant radius of pulley, which simplifies the kinematic mapping. Due to the absence of direct coupling between axes, the unified model becomes simple to simulate with a reduction in computational complexity.

Unlike the Cartesian configuration, the Polar configuration needs inverse kinematics to map workspace co-ordinates to motor rotations. For a polar printer, the angular and radial motions are dependent on each other, and the transformation from Cartesian to Polar co-ordinates involves trigonometric functions and square roots, which increase the model's nonlinearity. The unified model of polar includes a complex mathematical expression, involving the torque equation, the non-linear velocity profile, and time varying Jacobian function for coordinate transformation. Considering the above factor, complexity increases in the differential equation and induced stiffness in the system, which increases the computational load.

Table 1. Comparative Summary based on Mathematica approach

Criteria	Cartesian Printer	Polar Printer
Axis Coupling [4], [9]	Decoupled	Coupled (R and θ)
Kinematic Mapping [7], [15]	Linear	Non-Linear
Number of equations [4], [18]	Moderate	High
Controller Design [12], [15]	Modular	Integrated, Multi-Variable

Considering the model complexity of Cartesian and Polar 3D printer as shown in Table 1 the comparative analysis reveals the distinct advantages for each configuration. In the case of a Cartesian printer, decoupled axis and linear kinematics offer a simple unified model that is easy to simulate and control. This modular structure facilitates independent axis modelling that results in lower computational with high accuracy. Due to these reasons its ideally applicable where precision and ease of control are required. In the case of the Polar printer, being mechanically efficient and compact in nature, it makes modelling and controls challenging. The unified model for the polar printer is more complex, which requires inverse kinematics and coordinate control strategies. Polar printer excels in manoeuvring in circular or rotational manner their motion accuracy is compromises in critical trajectories.

3.2 Model complexity

In a Cartesian printer, the mathematical model is simple since all three axes i.e., X, Y, and Z, are decoupled. Each axis operates independently which means relation between motor rotation and head displacement is direct. Because of the simplicity of the controller allow the use of modular Proportional-Integral-Derivative (PID) loops for each axis without solving complex equations, resulting in less computational time, making the Cartesian printer suitable for real-time control and low-cost microcontroller. Polar printer has nonlinear and coupled kinematics between radial and angular axes. Controller compute inverse kinematics to change cartesian coordinate into R and Θ position with synchronize motion. This can only be done by solving the nonlinear differential equation and handling the coupling effect in real time, which leads to an increase in computational load. In conclusion can be made that a powerful processor's algorithm is required for smooth printing.

3.3 Print Pattern Complexity

Cartesian printer handles rectilinear path efficiently because straight lines and gird base infill require simple linear interpolation. On the contrary for smooth curve controller needs a piecewise linear approximation, which make computational at a manageable. Polar excel in circular and radial patterns, which align naturally with their kinematics. But the problem arises for irregular or rectangular shapes, where repetitive calculation for radial and angular axes is required. This increases the computational time, especially for intricate designs.

Table 2. Comparative Summary based on model and print pattern complexity

Criteria	Cartesian Printer	Polar Printer
Print Pattern Complexity [21], [22]	Low for grid, moderate for curves	Low for circles, high for irregular shapes
Controller Load [12], [18]	Lightweight, modular PID	Heavy, requires inverse kinematics
Computational Time [23]	Short, predictable	Longer, variable with pattern complexity

The Table 2 shows the metrics chosen to translate modelling difference into practical impact: model complexity and controller load reflects the computational effort suggested by decoupled linear kinematics (Cartesian) versus coupled nonlinear invers kinematics (Polar), while printing complexity and computational time capture how each natural coordinate system affects trajectory generation, rectilinear efficiency for Cartesian and radial/circular efficiency for polar, with increased burden for irregular shapes.

4 Conclusion

The study validates the performance between Polar and Cartesian printers with the help of integrated kinematic modelling. The Cartesian printer, because of linear kinematics and decoupled axes, gives superior linear positioning accuracy and computational efficiency. Its modular control needs simple PID loops, enabling real-time operation on a low-cost microcontroller and resulting in predictable short computational cycles, which are suitable for rectilinear patterns and intricate designs. Polar printer, on the contrary, due to compactness and radial efficient geometry, suffers from coupled and nonlinear dynamics. The inverse kinematics and real-time coordinate transformation increase computational load by 3-5 times, which requires a powerful processor, which leads to dynamic errors in irregularly shaped objects. Therefore, based on the application, a driven Cartesian printer is recommended for general-purpose and complex layer-based printers, while a polar configuration is best suited to concentric patterns. Actionable steps include developing polar path slicers that employee's model predictive control for polar systems and utilize the derived mathematical model as a DT for predictive virtual tuning and optimization that ensures precision to match geometric demands. Practically, this mathematical model enables predictive virtual tuning of control/motion parameters before printing, improving trajectory tracking under load and reducing trial and error calibration. Additionally, because the same nonlinear motor transmission foundation is reused across Polar and Cartesian configurations, it provides a base for future DT that integrates feedback for real-time monitoring, optimization, and adaptive control.

References

1) Marathe M. Mathematical Modelling and Motion Analysis of Cartesian and Polar 3D Printers Driven by Stepper Motors. *J Appl Nonlinear Dyn*. 2026. 10.5890/JAND.2026.03.001.
2) Rojek I, Marciniak T, Mikołajewski D. Digital Twins in 3D Printing Processes Using Artificial Intelligence. *Electronics*. 2024;13(17). 10.3390/electronics13173550.
3) Mourtzis D, Togias T, Angelopoulos J, Stavropoulos P. A Digital Twin architecture for monitoring and optimization of Fused Deposition Modeling processes. *Procedia CIRP*. 2021;103:97–102. 10.1016/j.procir.2021.10.015.
4) Yin M, Chen Y, Lee KH, Fu DKC, Tse ZTH, Kwok KW. Dynamic modeling and characterization of the core-Xy Cartesian motion system. *2018 IEEE Int Conf Real-Time Comput Robot RCAR 2018*. 2018;p. 206–211. 10.1109/RCAR.2018.8621684.
5) Raj A, et al. Optimization of Cartesian and polar 3D printer structures using finite element analysis: a comparative study on material selection and design enhancement. *Proc Indian Natl Sci Acad*. 2025;91(3):804–820. 10.1007/s43538-024-00363-1.
6) Bernardi F, Carfagna E, Migliazza G, Buticchi G, Immovilli F, Lorenzani E. Performance Analysis of Current Control Strategies for Hybrid Stepper Motors. *IEEE Open J Ind Electron Soc*. 2022;3:460–472. 10.1109/OJIES.2022.3185659.
7) Kopets E, Karimov A, Scalera L, Butusov D. Estimating Natural Frequencies of Cartesian 3D Printer Based on Kinematic Scheme. *Applied Sciences*. 2022;12(9). 10.3390/app12094514.
8) Cao G, Chen Z, Wang D, Zhao X, Meng F. A Robust Fuzzy Adaptive Control Scheme for PMSM with Sliding Mode Dynamics. *Processes*. 2025;13(8). 10.3390/pr13082635.
9) Tyagi B, et al. Modelling Structural Behaviour of the Cartesian, Polar, and Delta Material Extrusion Printers by Finite Element Analysis. *J Inst Eng Ser C*. 2024;105(3):617–634. 10.1007/s40032-024-01066-8.

10) Palanisamy S, Karuppiah G, Kumar P, Dharmalingam S, Mubarak S, Santulli C. Review Article Effect of Process Parameters and Material Selection on the Quality of 3D Printed Products by Fused Deposition Modeling (FDM): A Review. *Advances*. 2024. 10.1155/adv/3480281.
11) Mishra N, Singh SP. .
12) Simpkins A. .
13) Tlegenov Y, Lu WF, Hong GS. A dynamic model for current-based nozzle condition monitoring in fused deposition modelling. *Progress in Additive Manufacturing*. 2019;4(3):211–223. 10.1007/s40964-019-00089-3.
14) Zakharov O. Modeling and Analysis of Delta Kinematics FDM Printer. *Journal of Physics: Conference Series*. 2022 Jun. 10.1088/1742-6596/2182/1/012069.
15) Zhao A, Toudeshki A, Ehsani R, Sun JQ. Data-Driven Inverse Kinematics Approximation of a Delta Robot with Stepper Motors. *Robotics*. 2023;12(5). 10.3390/robotics12050135.
16) Chouaibi Y, Slimani F, Chebbi E, Affi Z, Romdhane L. .
17) Savaliya J, Gosai KG, Sidapara A, Parikh H, Pithadiya B, Pandya H. 3D Printer Movement Modelling Through Denavit–Hartenberg Theory and RoboAnalyzer. In: Triwiyanto T, Rizal A, Caesarendra W, editors. Proceedings of the 2nd International Conference on Electronics, Biomedical Engineering, and Health Informatics. Singapore. Springer Nature Singapore. 2022;p. 355–371. 10.1007/978-981-19-1804-9_28.
18) Bouzid R, Gritli H, Narayan J. ANN Approach for SCARA Robot Inverse Kinematics Solutions with Diverse Datasets and Optimisers. *Applied Computer Science*. 2024;29(1):24–34. 10.2478/acss-2024-0004.
19) Xu H, Rong X. Design and Application Research on Control System of 3D Printer Based on Multi-DOF Robotic Arm. 2024;4(6):363–372. 10.26855/acc.2023.12.004.
20) Xie R, Li Y, Yi Y. Inverse kinematic analysis of 6-axis robotic arm 3D printing system based on position and posture separation method. In: Chen L, Zain ABM, editors. Fourth International Conference on Electronic Information Engineering and Data Processing (EIEDP 2025). SPIE. 2025;p. 135743T. 10.1117/12.3067059.
21) Alba JCG, Nunez DA, Mauledoux M, Aviles OF. Deposition Toolpath Pattern Comparison: Contour-Parallel and Hilbert Curve Application. 2022;11(7):542–548. 10.18178/ijmerr.11.7.542-548.
22) Liu B, Lin Z, Xue Y, Sun Y, Fu J. Continuous hybrid zigzag and contour toolpath for additive manufacturing with sparse and adhered filling. *International Journal of Advanced Manufacturing Technology*. 2023;129(1):321–334. 10.1007/s00170-023-12257-5.
23) Gupta P, Guo Y, Boddeti N, Krishnamoorthy B. SFCDecomp: Multicriteria Optimized Tool Path Planning in 3D Printing using Space-Filling Curve Based Domain Decomposition. *International Journal of Computational Geometry & Applications*. 2021;31(4):193–220. 10.1142/S0218195921500096.
24) Series C. Mathematical modeling for resource and energy saving control of extruders in multi-assortment productions of polymeric films;vol. 1015. 2018. 10.1088/1742-6596/1015/3/032104.
25) Kamaraj AB, Sundaram M. A mathematical model of the deposition rate and layer height during electrochemical additive manufacturing. *International Journal of Advanced Manufacturing Technology*. 2019;102(5):2367–2374. 10.1007/s00170-019-03292-2.
26) Banerjee D, Mishra SB, Khan MS, Kumar MA. Mathematical approach for the geometrical deformation of fused deposition modelling build parts. *Materials Today: Proceedings*. 2020;33:5051–5054. 10.1016/j.matpr.2020.02.842.